

# *In vitro* anticancer effects of alpelisib against PIK3CA-mutated canine hemangiosarcoma cell lines

MARIKA MAEDA<sup>1</sup>, KAZUHIKO OCHIAI<sup>1,2</sup>, MASAKI MICHISHITA<sup>2,3</sup>, MASAMI MORIMATSU<sup>4</sup>, HIROKI SAKAI<sup>5</sup>, NAYUTA KINOSHITA<sup>4</sup>, MOTOHARU SAKAUE<sup>6</sup>, ERI ONOZAWA<sup>7</sup>, DAIGO AZAKAMI<sup>8</sup>, MASAMI YAMAMOTO<sup>9</sup>, KATSUMI ISHIOKA<sup>7</sup>, TAKUYA SADAHIRA<sup>10</sup>, MASAMI WATANABE<sup>10</sup> and YOSHIKAZU TANAKA<sup>1,2</sup>

<sup>1</sup>Laboratory of Veterinary Hygiene, School of Veterinary Science; <sup>2</sup>Research Center for Animal Life Science;

<sup>3</sup>Laboratory of Veterinary Pathology, Nippon Veterinary and Life Science University, Tokyo 180-8602;

<sup>4</sup>Laboratory of Laboratory Animal Science and Medicine, Graduate School of Veterinary Medicine, Hokkaido University, Sapporo, Hokkaido 060-0818; <sup>5</sup>Laboratory of Veterinary Pathology, Gifu University, Gifu 501-1193;

<sup>6</sup>Laboratory of Anatomy II, Department of Veterinary Medicine, Azabu University, Sagami-hara-shi, Kanagawa 252-5201;

<sup>7</sup>School of Veterinary Nursing and Technology, Nippon Veterinary and Life Science University, Tokyo 180-8602;

<sup>8</sup>Laboratory of Clinical Oncology, Tokyo University of Agriculture and Technology, Tokyo 183-8538; <sup>9</sup>Division of Physiological Pathology, Nippon Veterinary and Life Science University, Tokyo 180-8602; <sup>10</sup>Department of Urology, Graduate School of Medicine, Dentistry and Pharmaceutical Sciences, Okayama University, Okayama 700-0914, Japan

Received November 26, 2021; Accepted February 9, 2022

DOI: 10.3892/or.2022.8295

**Abstract.** Hemangiosarcoma (HSA) is a malignant neoplasm that occurs in humans and canines with a poor prognosis owing to metastatic spread, despite effective treatment. The frequency of spontaneous HSA development is higher in canines than in humans. Therefore, canine HSA is a useful model of intractable human disease, which requires early detection and an effective therapeutic strategy. A high frequency of the p110 $\alpha$  phosphatidylinositol-4,5-bisphosphate 3-kinase catalytic subunit alpha (PIK3CA) mutations is detected in a comprehensive genome-wide analysis of canine cases of HSA. The present study cloned the full-length cDNA of canine PIK3CA and identified a mutation in codon 1047 from canine cases of HSA and cell lines that were established from these. The enforced expression of the 1047th histidine residue (H1047) R or L mutants of canine PIK3CA in HeLa cells enhanced epidermal growth factor receptor (EGFR) signaling via Akt phosphorylation. PIK3CA mutant canine HSA cell lines exhibited the hyperphosphorylation of Akt upon EGF stimulation as well. Alpelisib, a molecular targeted drug against PIK3CA activating mutations, exerted a significant antitumor effect in

canine PIK3CA-mutated HSA cell lines. By contrast, it had no significant effect on canine mammary gland tumor cell lines harboring PIK3CA mutations. On the whole, the findings of the present study suggest that alpelisib may be highly effective against PIK3CA mutations that occur frequently in canine HSA.

## Introduction

Angiosarcomas in humans are rare, highly aggressive, malignant, endothelial cell tumors of vascular or lymphatic origin. Treatment is challenging in a number of cases, and the prognosis is poor (1). Canine hemangiosarcoma (HSA) is also an aggressive malignant neoplasm with a poor prognosis. Surgery and chemotherapy have had limited success in prolonging survival and increasing the quality of life of canines with HSA (2). HSA tissues overexpress vascular endothelial growth factor (VEGF), fibroblast growth factor (FGF) and their receptors (1,3). These growth factors generally induce tyrosine kinase activation of receptors and activate downstream signaling pathways, including the MAPK/ERK and phosphatidylinositol-3 kinase/Akt/mammalian target of rapamycin (PI3K/Akt/mTOR) pathways, which are involved in tumor progression (4-6). MAPK/ERK pathways in endothelial cells are activated in tumors (7-9). The PI3K/Akt/mTOR pathway also participates in the pathogenesis of endothelial cells (10,11). Phosphatase and tensin homolog (PTEN) mutation, which is an antagonist of PI3K, has been detected in human and canine HSA cases (12,13), and the hyperactivation of the Akt/mTOR pathway has been reported in sporadic human HSA cases (14). However, the role of the PI3K/Akt/mTOR pathway in canine HSA has not yet been well investigated (15).

HSA occurs in ~50,000 canines per year in the United States (16), and its frequency is higher than that in humans,

*Correspondence to:* Dr Kazuhiko Ochiai, Laboratory of Veterinary Hygiene, School of Veterinary Science, Nippon Veterinary and Life Science University, 1-7-1 Kyonan-cho, Musashino, Tokyo 180-8602, Japan

E-mail: kochiai@nvl.u.ac.jp

**Key words:** Akt, alpelisib, canine, hemangiosarcoma, mutation, p110 $\alpha$  phosphatidylinositol-4,5-bisphosphate 3-kinase catalytic subunit alpha

rendering this a useful model for the study of human intractable disease that requires early detection and effective therapeutic strategy. Developments in genome-wide approaches have enabled the comprehensive analysis of disease-related gene mutations in humans and animals (17,18). Mutated canine genes related to HSA have been searched using exome sequencing, and the 1047th histidine residue (H1047) of p110 $\alpha$  phosphatidylinositol-4,5-bisphosphate 3-kinase catalytic subunit alpha (PIK3CA) was found to be highly mutated (19). PIK3CA acts downstream of the EGFR pathway. In human tumor cases, mutations of the 1047th histidine (e.g., H1047R and H1047L) of PIK3CA have been shown to induce the hyperactivation of EGFR signaling. Akt phosphorylation and tumor cell proliferation are enhanced by this mutation (20). The importance of the PIK3CA mutation in canine HSA is well recognized; however, the open reading frame of canine PIK3CA has not yet been cloned, at least to the best of our knowledge. The present study thus cloned canine PIK3CA and produced mutants by substituting the H1047 residue and investigated functional alterations in EGFR signaling via Akt phosphorylation. The anti-proliferative effects of alpelisib, which suppresses the hyperactivation of EGFR signaling by the PIK3CA mutation (21), on canine HSA cell lines were also investigated.

## Materials and methods

*cDNA cloning, sequencing and mutagenesis of canine PIK3CA.* cPIK3CA was amplified by polymerase chain reaction (PCR) using the following oligonucleotide primers: cPIK3CA-F (5'-CTGGGACCCGATGTGGTTAGAG-3') and cPIK3CA-R (5'-GAAATGAACTAGTTTGTGCTC-3'). These primers were designed based on canine-predicted canine PIK3CA (cPIK3CA) sequences (GenBank accession no. XM\_022414352.1). RNA was obtained from canine total kidney RNA (Zymo Research Corp.). The total RNA (4  $\mu$ g) was denatured at 70°C for 10 min, cooled immediately, and reverse transcribed, using 200 units of SuperScript III (Thermo Fisher Scientific Inc.), 25 pmol of random primer, and 10 nmol dNTPs in total volume of 20  $\mu$ l at 37°C for 50 min. PCR amplification was performed using PrimeSTAR (Takara Bio, Inc.). PCR was conducted for 30 cycles, each consisting of denaturation at 96°C for 30 sec, annealing at 55°C and extension at 72°C for 3 min. Sequence data were determined for at least five independent clones using an ABI 3730 platform (Applied Biosystems; Thermo Fisher Scientific Inc.). For sequence analysis, human PIK3CA (GenBank accession no. NP\_006209.2) and cPIK3CA (GenBank accession no. LC625864.1) were compared using Genetyx software ver. 15 (Genetyx Corporation) (Fig. S1). dATP was added to the PCR products using a 10X A-attachment kit (Toyobo Life Science) and cloned into pGEM-T Easy (Promega Corporation). To construct the H1047R and H1047L mutants, nucleotide substitutions were performed by PCR mutagenesis using a pGEM-T Easy vector carrying the wild-type (WT) sequence as the template and the following oligonucleotide primers: cPIK3CA-H1047R-F (5'-GAATGATGCACGTCATGG TGGCTG-3'), cPIK3CA-H1047R-R (5'-CAGCCACCATGA CGTGCATCATTC-3'), cPIK3CA-H1047L-F (5'-GAATGA TGCACCTTCATGGTGGCTG-3') and cPIK3CA-H1047L-R

(5'-CAGCCACCATGAAGTGCATCATTC-3'). These clones were subcloned into the Halo-tagged expression vector pFN21A (Promega Corporation) containing *SgfI/PmeI* sites.

*Canine cell lines, formalin-fixed and paraffin-embedded (FFPE) tissue sample preparation and sequencing.* Genomic DNA of canine cell lines or FFPE tissues from paraffin scrolls (Table SI) was extracted from canine tumor samples using the ReliaPrep™ gDNA Tissue Miniprep System (for cell lines: Promega Corporation) or QIAamp DNA FFPE Tissue kit (for FFPE samples: Qiagen GmbH) following the manufacturer's instructions, respectively. PCR amplification was performed using PrimeSTAR (Takara Bio, Inc.). PCR was conducted for 30 cycles, each consisting of denaturation at 96°C for 30 sec, annealing at 55°C and extension at 72°C for 1 min. The primer pairs used for amplifying and sequencing canine cPIK3CA exon 21 were 5'-CTCAATGATGCTTGGCTCTGG-3' and 5'-CTAATGCTGTTTCATGGATTGTG-3'.

*Histological analysis.* With permission from the University Ethics Committee, we obtained tissue samples from the Department of Veterinary Pathology, School of Veterinary Science, Nippon Veterinary and Life Science University (approval no. 11-50, May 27, 2018). All samples were classified by veterinary pathologists in accordance with the World Health Organization classification (22) (Table SI). FFPE cancer tissues were sliced at a thickness of 4  $\mu$ m and the sections were placed on slides, following which hematoxylin and eosin (H&E) staining was performed. Tissues resected were fixed in 10% neutral buffered formalin for 24 h at 25°C, processed routinely and embedded in paraffin wax. FFPE cancer tissues were sliced at a thickness of 4  $\mu$ m and the sections were placed on slides, following which hematoxylin and eosin (H&E; Muto pure chemicals, Tokyo, Japan) staining was performed. H&E sections were examined using a light microscope (BX53, Olympus Corporation).

*Cells and cell culture.* HeLa cells were purchased from the American Type Culture Collection (ATCC). Canine mammary gland tumor (CMT) and HSA cell lines were established and characterized in previous studies (15,23). The HeLa cells and CMT cell lines were maintained in Dulbecco's modified Eagle's medium (FUJIFILM Wako Pure Chemical Corporation), and HSA cell lines were maintained in RPMI-1640 medium (FUJIFILM Wako Pure Chemical Corporation), supplemented with 10% fetal bovine serum, penicillin and streptomycin (FUJIFILM Wako Pure Chemical Corporation) and incubated at 37°C in a 5% CO<sub>2</sub> atmosphere.

*Transfections.* HeLa cells (2x10<sup>5</sup>/well in 6-well plates, 500  $\mu$ l medium/well) were transfected with 1  $\mu$ g pFN21A vector (Promega Corporation) containing cPIK3CA WT or H1047R-L mutant plasmids using FuGENE HD Transfection Reagent (Promega Corporation). An empty pFN21A vector was transfected as a control. At 48 h (37°C incubation) after the cells were transfected, they were used for western blot analysis.

*Stimulation with anticancer agents and EGF stimulation for Akt phosphorylation.* Following a 24 h-incubation at 37°C, the cells were arranged in 6-well plates at a concentration

of  $2 \times 10^5$  cells/well. The medium was replaced with alpelisib (LC Laboratories) or doxorubicin (FUJIFILM Wako Pure Chemical Corporation) at suitable concentrations (alpelisib: 0, 1, 2, 5, 10, 20, 50 and 100  $\mu\text{M}$ ; doxorubicin: 0, 0.1, 0.5, 1, 5, 10 and 50  $\mu\text{M}$ ) followed by incubation for 24 h at 37°C, following which the cells were treated with EGF (PeproTech, Inc., 100 ng/ml) for 30 min.

**Western blot analysis.** Cells that were treated with EGF and/or drugs were lysed with mammalian lysis buffer (Promega Corporation) supplemented with a protease inhibitor cocktail (Promega Corporation). Protein concentrations were determined using a BCA protein assay kit (Nacalai Tesque). The protein extract from the cells (10  $\mu\text{g}$ ) was mixed with 2X loading buffer and separated on 5-20% gradient SDS-PAGE [Dream Realization and Commucation (DRC); <https://www.drc2002.com/index.html>]. The separated proteins were transferred to polyvinylidene difluoride (PVDF) membranes. The membranes were blocked with EzBlock Chemi reagent (ATTO Corporation) for 1 h at 25°C. Western blot analysis was performed using the following primary antibodies for 16 h at 4°C: Rabbit polyclonal anti-Halo (1:1,000; cat. no. G9281, Promega Corporation), rabbit monoclonal anti-Akt (Pan; 1:1,000; cat. no. 4691), p-Akt (Ser473; 1:1,000; cat. no. 4060), Akt1 (1:1,000; cat. no. 2938, CST), Akt2 (1:1,000; cat. no. 3063), p-Akt1 (1:1,000; cat. no. 9018) p-Akt2 (1:1,000; cat. no. 8599) (all from Cell Signaling Technology, Inc.) and mouse monoclonal anti- $\alpha$ -tubulin (1:2,000; cat. no. 013-25033, FUJIFILM Wako Pure Chemical Corporation). Horseradish peroxidase-conjugated secondary antibodies for 1 h at 25°C and EzWestLumi plus (ATTO Corporation) were used to detect antibody-bound proteins, and band intensities were quantified by densitometry using ImageJ ver. 1.53e software (National Institutes of Health).

**MTT assay.** The cytotoxic effects of alpelisib and doxorubicin were evaluated using MTT assay. The cells were plated in 96-well plates at a density of  $5 \times 10^3$  cells/well. After 24 h, the medium was replaced with 75  $\mu\text{l}$  medium containing alpelisib or doxorubicin at various concentrations (0, 0.1, 0.5, 1, 5, 10 and 50  $\mu\text{M}$ ) and incubated for 24, 48 or 72 h at 37°C. At the end of the treatment period, 7.5  $\mu\text{l}$  MTT (5 mg/ml PBS) was added to each well. The cells were then incubated for 4 h at 37°C in an incubator (WAKENYAKU Co., Ltd.). The colored crystals of the produced formazan crystals were dissolved in 150  $\mu\text{l}$  DMSO. The purple blue formazan formed was measured using a MULTISKAN FC (Thermo Fisher Scientific, Inc.) at 570 nm. The optical density of each sample was compared with the control optical density, and graphs were plotted using SkanIt™ Software ver. 4.1 (Thermo Fisher Scientific, Inc.). IC<sub>50</sub> values were obtained from the generated inhibition curve plots.

**Tumor cell migration assay.** The inhibition of HSA cell migration with alpelisib was assessed using a wound healing assay (24). HSA cells were seeded in RPMI-1640 medium (FUJIFILM Wako Pure Chemical Corporation), supplemented with 10% fetal bovine serum, penicillin and streptomycin (FUJIFILM Wako Pure Chemical Corporation) and grown in confluent monolayers in 6-well plates at a density of

$4 \times 10^5$  cells/well for 24 h. A single scratch wound was created using a sterile micropipette tip. Subsequently, the cell debris was removed by washing the plates twice with PBS, and the cell culture medium was refreshed with or without 20  $\mu\text{M}$  alpelisib. The cells were cultivated for up to 8 h. Three independent experiments were performed, and the area of cell migration was examined using an inverted microscope (DM IL LED, Leica Microsystems) and quantified using ImageJ ver. 1.53e software (National Institutes of Health).

**Caspase-3/7 activity assay.** The HSA cell lines were seeded in 96-well plates at a concentration of  $1 \times 10^4$  cells/well and treated with DMSO as a vehicle for alpelisib at 5 or 20  $\mu\text{M}$  and incubated for 24 h at 37°C. Caspase-3/7 activity was measured using the Caspase-Glo 3/7 Assay (Promega Corporation) according to the manufacturer's instructions. Luminescence was measured using a GloMax 96 microplate luminometer (Promega Corporation). Caspase-3/7 activities following alpelisib treatment are shown as relative values to those following treatment with the vehicle (DMSO).

**Statistical analysis.** Data are expressed as the mean  $\pm$  standard deviation. Analysis of variance with Tukey's post hoc test were used when multiple comparisons were required. A value of  $P < 0.01$  was considered to indicate a statistically significant difference.

## Results

**Isolation of the H1047R and H1047L mutations from canine HSA.** Genomic DNA was isolated from tumor FFPE samples from 19 canine HSA samples. PCR amplification of exon 21 of cPIK3CA containing the 3140th nucleotide coding H1047 revealed two genetic alternations in samples 7 and 9. Sample 7 exhibited a definite heterozygous 3140 A/G peak, wherein histidine was replaced with arginine at residue 1407 (H1407R) (Fig. 1A). On the other hand, sample 9 exhibited a minimal 3140 A/T peak (Fig. 1B). When this PCR product was cloned and sequenced, the 3140T clone was confirmed, in which histidine was replaced with leucine at residue 1407 (H1407L) (Fig. 1B). No other somatic mutations in H1047 of cPIK3CA were found in these samples. Representative H&E-stained normal (Fig. 1C) and HSA samples (Fig. 1D and E) with H1047R (case no. 7 in Table SI) or H1047L (case no. 9) are shown. Microscopically, the neoplasm was composed of neoplastic endothelial cells with large round-to-oval nuclei that form irregular vascular channels compared to normal vascular channels.

**The enforced expression of PIK3CA mutants induces the hyperphosphorylation of Akt in HeLa cells.** The Halo-tagged (WT: 1047H) and mutant (1047R or 1047 L) of cPIK3CA were forcibly expressed into HeLa cells. Both 1047R and 1047L mutants induced the hyperphosphorylation of Akt with/without EGF stimulation compared to the untransfected cells and WT-transfected cells (Fig. 2). In particular, Akt2 was phosphorylated by cPIK3CA mutant transfection.

**Seven of eight of canine HSA cell lines have mutated alleles that code 1047L.** Exon 21 of PIK3CA from eight canine cell lines (JuA1, JuB2, JuB2-1, JuB4, Re12, Re21, Ud2 and Ud6),

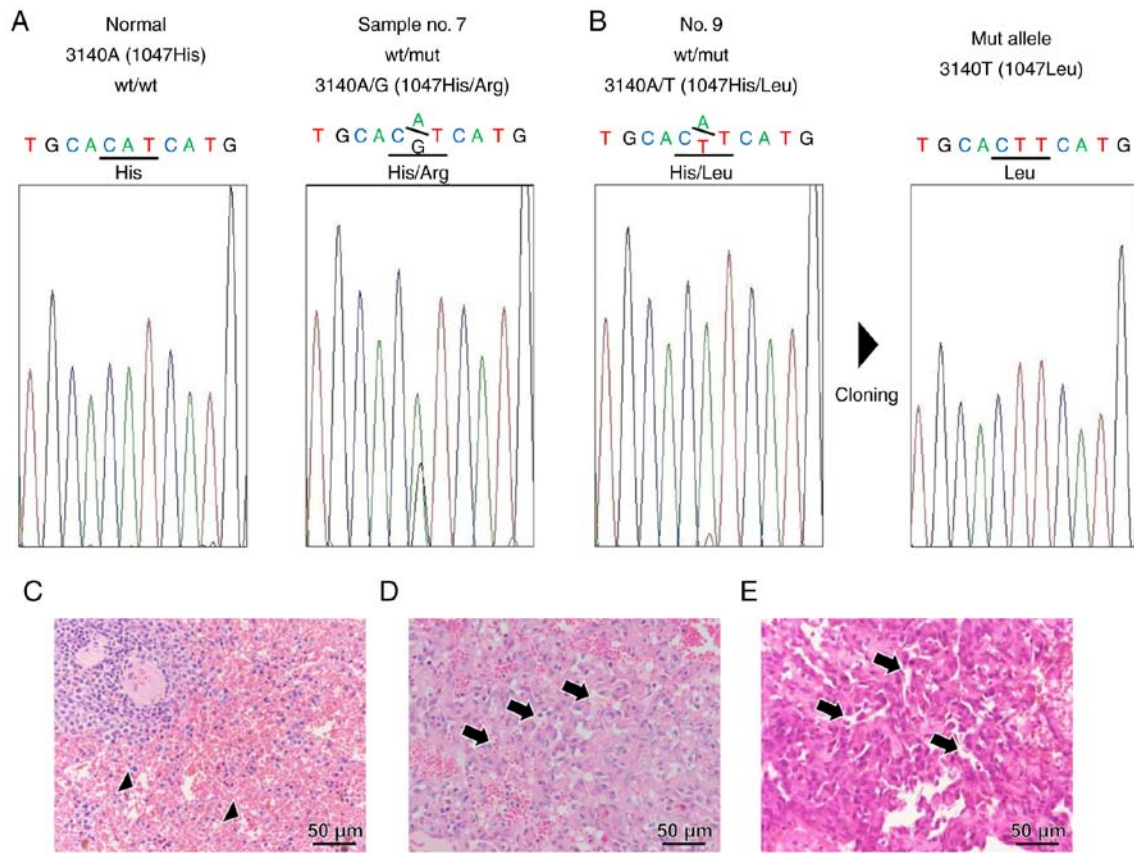


Figure 1. Detection of canine PIK3CA 3140A (1047His) mutation. (A) Electropherograms of Sanger sequencing of canine PIK3CA. Normal sample exhibited homozygous 3140A (1047His) peak (left panel). HSA sample no. 7 exhibited articulated heterozygous 3140A/G (H1047R) peak. (right panel). (B) HSA sample no. 9 exhibited minimal 3140A>T (H1047L) peak (left panel). One of the cloned samples shows 3140T (H1047L) peak (right panel). Photomicrographs of canine (C) normal spleen, (D) no. 7, (E) and no. 9 HSA samples. HSA tissues show representative pathogenesis as indicated by hematoxylin and eosin staining. The normal vascular channels are indicated by arrowheads, and irregular vascular channels are indicated by arrows. Scale bar, 50  $\mu$ m. PIK3CA, p110 $\alpha$  phosphatidylinositol-4,5-bisphosphate 3-kinase catalytic subunit alpha; HSA, hemangiosarcoma.

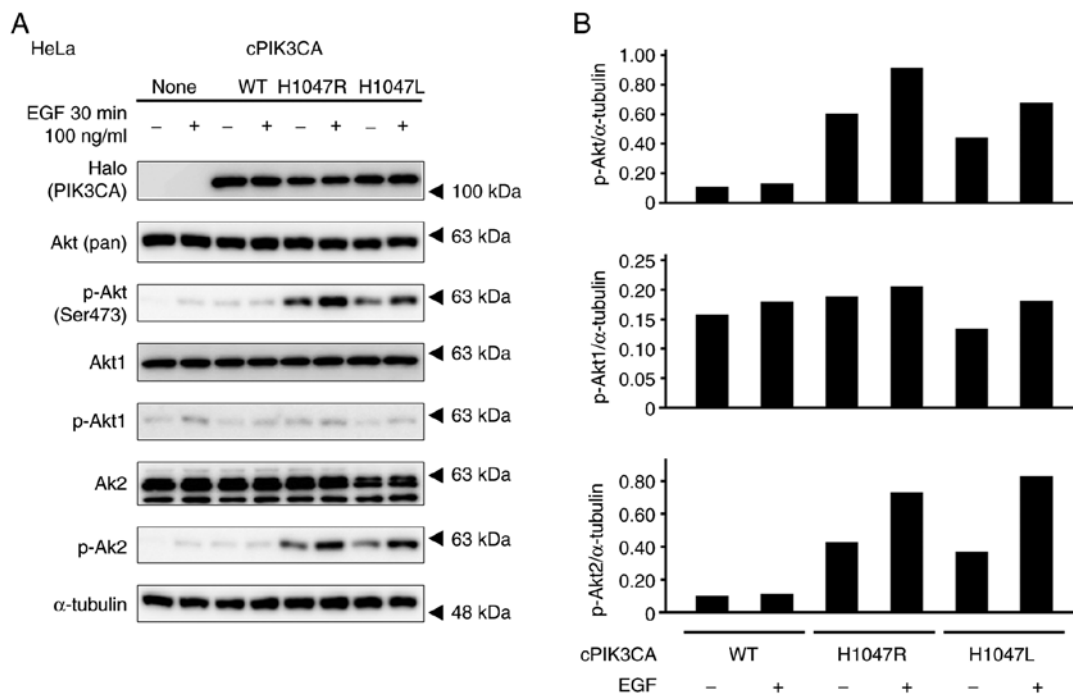
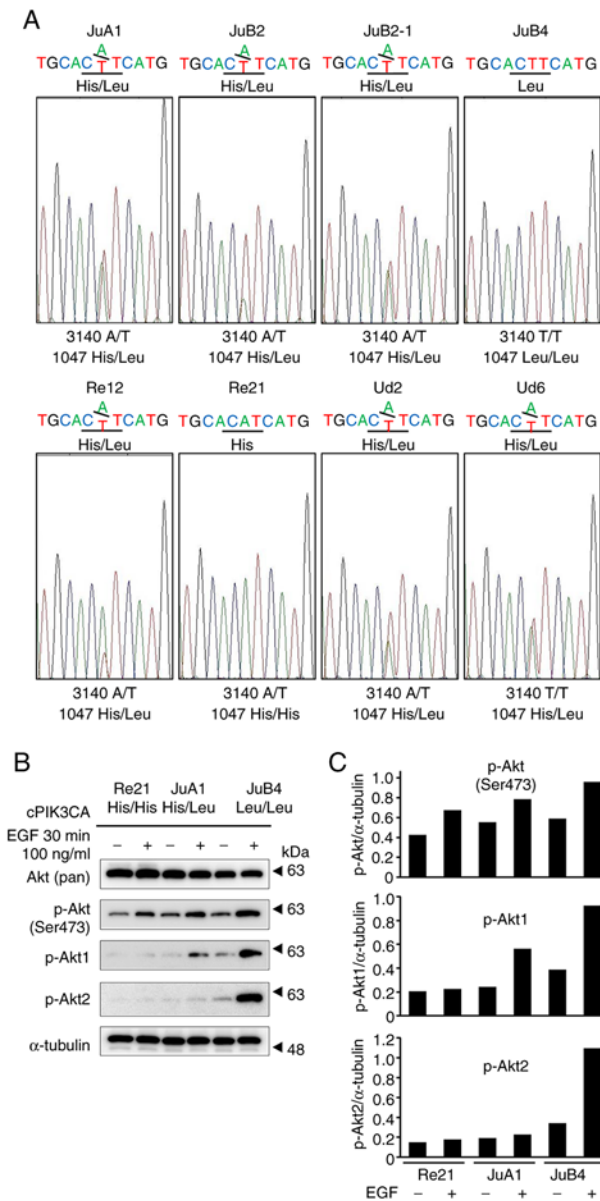


Figure 2. Phosphorylation profiles of Akt of HeLa cells with the enforced expression of PIK3CA mutants, which were stimulated with 100  $\mu$ M EGF for 30 min. (A) Expression levels of Halo-tagged PIK3CA, Akt (pan), p-Akt (Ser473), Akt1, p-Akt1, Akt2, and p-Akt2 were determined by western blotting.  $\alpha$ -tubulin was used as a loading control. (B) Graphs depict densitometric analysis of the western blots. The intensities of the p-Akt, p-Akt1, and p-Akt2 bands were quantified by densitometry and normalized to those of  $\alpha$ -tubulin. PIK3CA, p110 $\alpha$  phosphatidylinositol-4,5-bisphosphate 3-kinase catalytic subunit alpha.



**Figure 3.** PIK3CA mutation profile of eight canine HSA cell lines and phosphorylation profile with EGF stimulation. (A) Electropherograms of Sanger sequencing of PIK3CA of 8 canine HSA cell lines. (B) Expression levels of Akt (pan), p-Akt (Ser473), p-Akt1 and p-Akt2 examined using western blot analysis.  $\alpha$ -tubulin was used as a loading control. (C) Graphs depict densitometric analysis of the western blots. The intensities of the p-Akt, p-Akt1 and p-Akt2 bands were quantified by densitometry and normalized to those of  $\alpha$ -tubulin. PIK3CA, p110 $\alpha$  phosphatidylinositol-4,5-bisphosphate 3-kinase catalytic subunit alpha; HSA, hemangiosarcoma.

which were established from canine spontaneous HSA cases, were PCR-amplified and directly sequenced (15). Apart from Re21, the JuA1 cells had a 1047L heterozygous mutation and the JuB4 cells had a homozygous 1047L mutation (Fig. 3A). Following stimulation with 100 ng/ $\mu$ l EGF in three different representative cell lines [Re21 (1047H/H WT), JuA1 (1047H/L heterozygous) and JuB4 (1047 L/L homozygous)] for 30 min, all three cell lines exhibited the hyperphosphorylation of Akt at Ser473 (Fig. 3B and C). The JuB4 cells exhibited the phosphorylation of both Akt1 and Akt2 upon EGF stimulation. By contrast, the JuA1 cells exhibited only Akt1 phosphorylation upon EGF stimulation (Fig. 3B and C).

*Inhibitory effects of alpelisib on the proliferation of canine HSA cell lines.* Canine HSA cell lines were treated with increasing concentrations of alpelisib (0, 1, 2, 5, 10, 20, 50 and 100  $\mu$ M) for 24, 48 and 72 h. The PIK3CA-mutant cell lines (JuA1 and JuB4) were more sensitive to alpelisib, with a decrease in cell proliferation observed in a concentration-dependent manner, compared with the PIK3CA WT cell line (Re21) at 48 and 72 h following alpelisib treatment, but not at 24 h (Fig. 4A-C). The IC<sub>50</sub> values of the PIK3CA-mutant cell lines were 11.26  $\mu$ M (48 h) and 7.39  $\mu$ M (72 h) for the JuA1 cells, and 19.62  $\mu$ M (48 h) and 18.23  $\mu$ M (72 h) for the JuB4 cells. The PIK3CA WT cell line exhibited higher IC<sub>50</sub> values for alpelisib treatment (IC<sub>50</sub> values: 52.85  $\mu$ M at 48 h, 26.63  $\mu$ M at 72 h). By contrast, the Re21 cell line was inhibited more effectively by doxorubicin treatment than the JuA1 and JuB4 cells (Fig. 4D). Akt phosphorylation at Ser473 was markedly inhibited by alpelisib treatment in the JuA1 cells and moderately inhibited in the JuB4 cells (Fig. 4E and F). On the other hand, the Re21 cells exhibited Akt Ser473 phosphorylation following alpelisib treatment. The phosphorylation analysis of p-Akt1 and p-Akt2 revealed that the JuA1 cells exhibited decreased p-Akt1 and p-Akt2 levels.

*Alpelisib inhibits cell migration.* At 8 h after scratching without alpelisib treatment, all cell lines recovered completely (Fig. 5A, lower left panels of cell lines, respectively). However, with 20  $\mu$ M alpelisib treatment, only the Re21 cells recovered almost completely from the wound after 8 h; the JuA1 and JuB4 cells exhibited a significantly delayed wound healing ability (Fig. 5B).

*Alpelisib induces caspase-3/7 activities in PIK3CA mutant cells.* The cells were exposed to alpelisib at a range of concentrations (0, 5 or 20  $\mu$ M) for 24 h; the Re21 cells did not exhibit an increase in caspase-3/7 activity, while the PIK3CA mutant JuA1 and JuB4 cell lines exhibited a significant increase in caspase-3/7 activity following treatment with 5 and 20  $\mu$ M alpelisib (Fig. 5C).

## Discussion

The present study demonstrates that there are mutations in PIK3CA H1047 in both canine HSA cases and cell lines. In humans, the PIK3CA H1047th residue is mutated in a number of types of tumors (25). Although canine PIK3CA is also mutated in mammary gland tumor and hemangiosarcoma cases (19,26), the cloning and molecular characterization of canine PIK3CA have not yet been performed, at least to the best of our knowledge. Therefore, the present study cloned and characterized canine PIK3CA. The novel cloned canine PIK3CA (GenBank accession no. LC625864) exhibited a high homology with human PIK3CA (NP\_006209.2), and functional domains were well conserved (Fig. S1). The H1047 residue was conserved in canine PIK3CA in the same position. These structural properties suggest that canine PIK3CA possesses EGFR signaling activities.

In the mutation analysis of 19 cases of canine PIK3CA in HSA FFPE samples, either a H1047R or H1047L heterozygous mutation was detected. Although the 3140A>G (case no. 7: H1047R) mutant sequence waveform was absent, a small

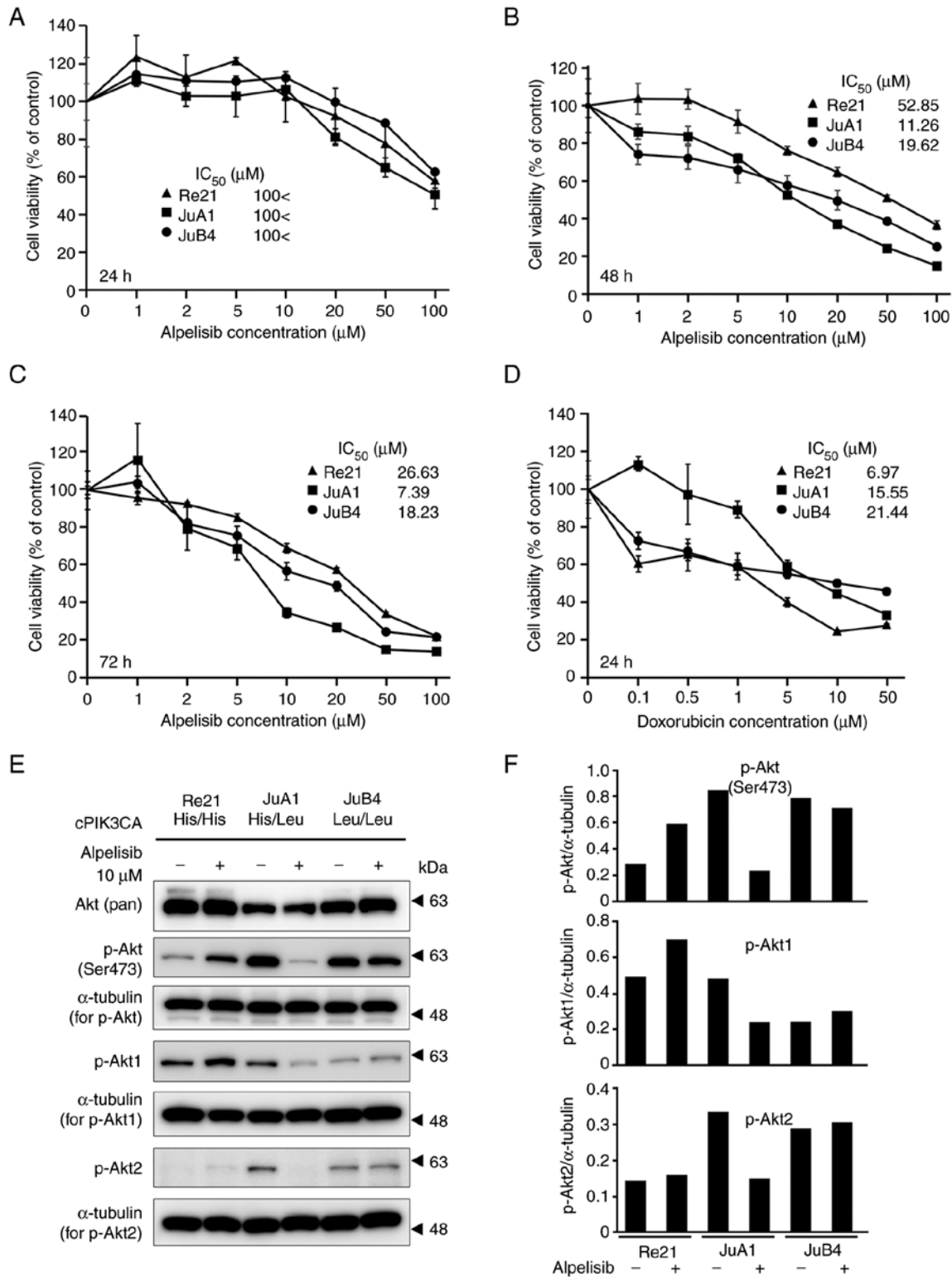


Figure 4. Anti-proliferative activity of alpelisib in canine HSA cell lines. PIK3CA wild-type or heterozygous/homozygous mutant cell lines were treated with increasing concentrations of alpelisib (0, 1, 2, 5, 10, 20, 50 and 100  $\mu\text{M}$ ) for (A) 24, (B) 48 and (C) 72 h. Cells were also treated with doxorubicin (0, 0.1, 0.5, 1, 5, 10 and 50  $\mu\text{M}$ ) for 24 h (D). The  $\text{IC}_{50}$  values and cell viability using an MTT assay were determined by measuring the absorbance at 560 nm on a microplate reader. The values of no treatment were 100%, and the values are shown from four independent experiments as the mean  $\pm$  SD. (E) Western blot analysis of Akt phosphorylation in canine HSA cell lines with 10  $\mu\text{M}$  alpelisib treatment for 6 h. (F) Graphs depicting densitometric analysis of the western blots compared with the loading controls. The intensities of the p-Akt, p-Akt1, and p-Akt2 bands were quantified through densitometry and normalized to the intensity of  $\alpha$ -tubulin. PIK3CA, p110 $\alpha$  phosphatidylinositol-4,5-bisphosphate 3-kinase catalytic subunit alpha; HSA, hemangiosarcoma.

waveform of 3140A>T (case no. 9: H1047L) was detected. This mutant could be cloned and confirmed; however, there may be other invisible mutants in other cases. It has been

previously reported that the detection limit of rare alleles by Sanger sequencing is  $\sim 10\%$  (27). High-resolution methods (e.g., pyrosequencing and next-generation sequencing) may

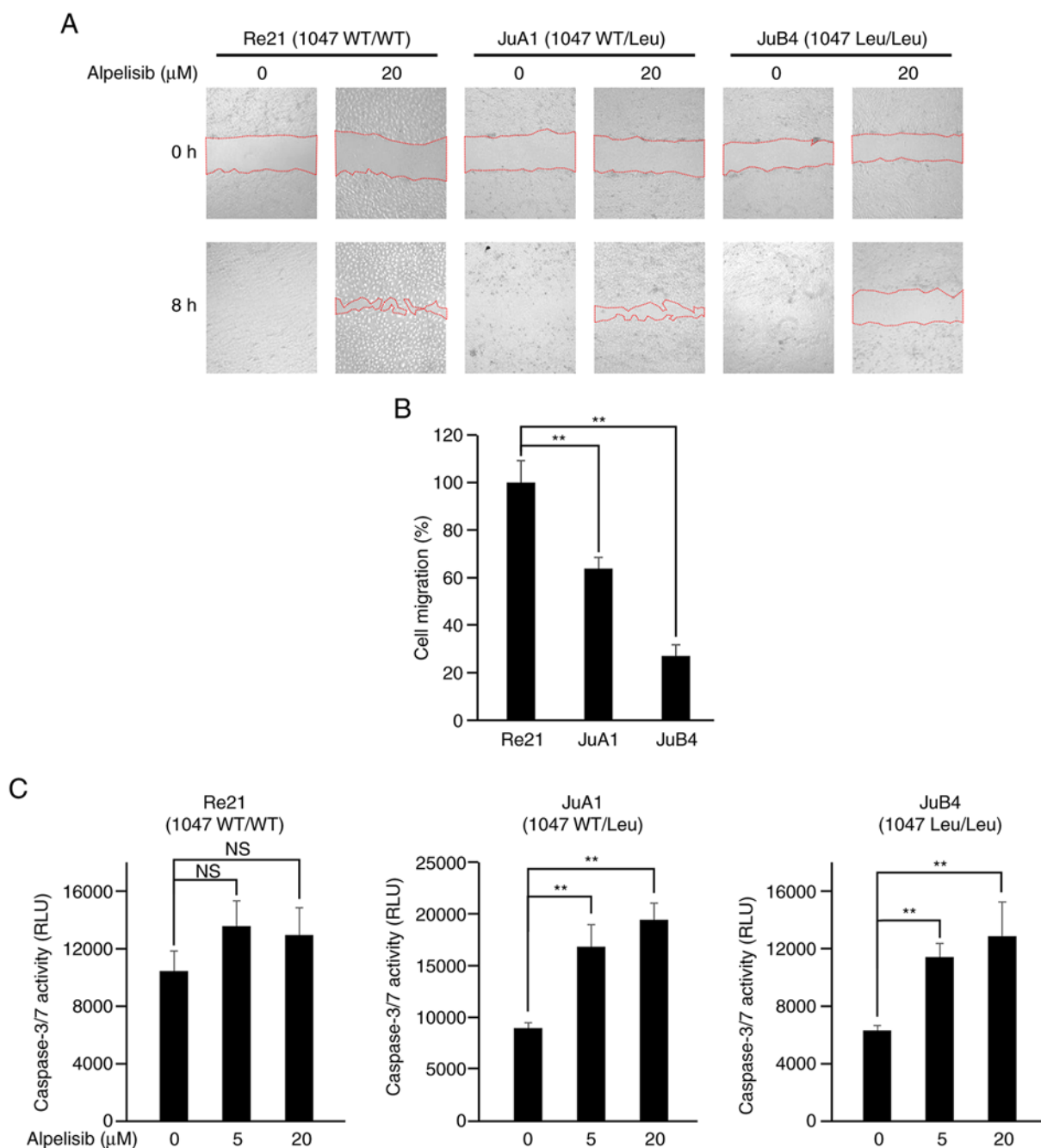


Figure 5. Anti-proliferative effects of alpelisib on canine HSA cell migration, and apoptosis induction via the activation of caspase-3/7. (A) The migration of canine HSA cell lines was assessed by the wound healing assay after 8 h of treatment. Representative images of the scratched areas are shown. Microscope magnification,  $\times 200$ . (B) Cell migration was quantified using ImageJ software. The values of cell migration of Re21 are 100%, and the values are shown from four independent experiments as the mean  $\pm$  SD. (C) Caspase-3/7 activity (RLU, relative luminescence units) was quantified 24 h after 5 or 20  $\mu\text{M}$  alpelisib treatment. The values are shown from three independent experiments as the mean  $\pm$  SD. Asterisks on top of the brackets indicate significant differences calculated by ANOVA with Tukey's multiple-comparison test (\*\* $P < 0.01$ ). NS, not significant; HSA, hemangiosarcoma; WT, wild-type.

be able to detect mutations in the 1047th residue of canine PIK3CA, which was isolated from tumor tissues (28,29). A definite pathological difference between the presence or absence of PIK3CA 1047th residue mutation was not detected by microscopic observation.

The analysis of Akt phosphorylation with the enforced expression of canine PIK3CA WT or H1047 mutants in HeLa cells revealed that H1047R- and H1047L-transfected cells exhibited the hyperphosphorylation of Akt; in particular, Akt2 but not Akt1 was phosphorylated with or without EGF

stimulation. In the human mammary tumor cell line, MCF10A, the enforced expression of H1047R of human PIK3CA mutant was previously shown to specifically induce Akt2 phosphorylation (30,31). The Akt isoforms Akt1 and Akt2 play differential roles in tumor metastasis (32). Akt1 has been demonstrated to suppress, while Akt2 promotes breast cancer cell migration and invasion *in vitro* (33). This result suggests that the canine PIK3CA H1047 mutation induces the upregulation of EGFR signaling and may promote tumor growth and invasion via Akt2 phosphorylation in HeLa cells.

Canine cell lines established from HSA or mammary gland tumor tissue were highly mutated in the H1047th residue of PIK3CA (Fig. S2). Herein, the overexpression of the canine PIK3CA H1047 mutation induced the phosphorylation of Akt2, but not Akt1 in HeLa cells. Alternatively, EGF stimulation induced the phosphorylation of endogenous canine Akt at Ser473 in the canine HSA cell lines, Re21, JuA1, and JuB4. JuA1 and JuB4, which were heterozygous/homozygous for the PIK3CA H1047L mutation, and induced the phosphorylation of Akt1 upon EGF stimulation, but not in the PIK3CA normal cell line, Re21. Given that only JuB4 exhibited Akt2 phosphorylation, a homozygous H1047L mutation may induce a stronger gain-of-function in PIK3CA. In canine HSA cell lines, the H1047L mutation of PIK3CA induced the phosphorylation of Akt1 and/or Akt2 with EGF stimulation, which may result in a severe pathogenesis (34).

Alpelisib (BYL719) is a targeted compound against mutated PIK3CA and is ~50-fold stronger than other isoforms (35). In the present study, alpelisib inhibited cell proliferation by suppressing Akt phosphorylation and inducing apoptosis via the activation of caspase-3/7 pathways, particularly in PIK3CA-mutant canine HSA cell lines. In MTT assays of canine HSA cell lines exposed to alpelisib, the JuA1 cell line, which is heterozygous for the H1047L mutation, was the most sensitive, although the JuB4 cell line, which is homozygous for the H1047L mutation, exhibited moderate sensitivity to alpelisib. JuA1 cells exhibited higher viability than JuB4 cells in a previous study (15). Thus, alpelisib may exert a potent antitumor effect on PIK3CA mutant tumor cells, which have a higher proliferative capacity, by suppressing Akt phosphorylation. On the other hand, although alpelisib also suppressed Akt phosphorylation in PIK3CA mutant cell lines, which were derived from canine mammary gland tumors (23), there was no marked difference in the tumor suppressive effect between normal and mutant PIK3CA cells (Fig. S2). Additionally, 20  $\mu$ M alpelisib also significantly inhibited cell migration in PIK3CA mutant cell lines compared with PIK3CA WT cell lines. It has been reported that canine HSA cells promote migration by interacting with CXCR4 and CXCL12 (36-38), and the overexpression of CXCR4 promotes the invasion and migration of non-small cell lung cancer via EGFR (39). These phenomena suggest that the suppression of abnormal EGFR signaling, induced by PIK3CA mutation, by alpelisib may be able to control canine HSA progression. Furthermore, alpelisib induced significant apoptotic cell death specifically in PIK3CA mutant canine HSA cell lines via caspase-3/7 activation; thus, alpelisib can be used as an agent for the treatment of canine HSA. In addition to the tumor-suppressive effect on canine PIK3CA mutant HSA *in vivo*, alpelisib has been confirmed to be safe for use in dogs based on safety examinations during drug development processes (e.g., [https://www.ema.europa.eu/documents/assessment-report/piqray-epar-public-assessment-report\\_en.pdf](https://www.ema.europa.eu/documents/assessment-report/piqray-epar-public-assessment-report_en.pdf)). Therefore, the authors aim to investigate its direct clinical effects on canine HSA cases in future studies.

In conclusion, the present study detected a PIK3CA H1047 mutation in canine HSA tissues and cell lines derived from canine HSA cases. The H1047R and H1047L mutations in canine PIK3CA induced EGFR signaling via Akt hyperphosphorylation. Alpelisib suppressed Akt phosphorylation, cell viability and migration, and induced apoptosis (determined by caspase-3/7 activation) in PIK3CA mutated canine HSA cell lines. These

data suggest that the H1047 mutation of PIK3CA is a crucial and useful marker of canine HSA, and alpelisib may prove to be an effective agent against PIK3CA-mutant canine HSA.

### Acknowledgements

Not applicable.

### Funding

The present study was supported by KAKENHI scientific research grants from the Ministry of Education, Culture, Sports, Science, and Technology of Japan (nos. 18H02334 and 19K06390).

### Availability of data and materials

The datasets used and/or analyzed during the current study are available from the corresponding author on reasonable request.

### Authors' contributions

KO, MMi, HS, KI, MW and YT designed the study. MMa, MMo, NK, MS, DA, MY, EO and TS performed the laboratory experiments. KO was responsible for the statistical analysis and wrote the manuscript. MW, YT, KI and KO supervised the study. KO, MMi and YT confirm the authenticity of all the raw data. All authors have read and approved the final version of the manuscript.

### Ethics approval and consent to participate

With permission from the University Ethics Committee of Nippon Veterinary and Life Science University, tissue samples were obtained from the Department of Veterinary Pathology, School of Veterinary Science, Nippon Veterinary and Life Science University (approval no. 11-50, May 27, 2018).

### Patient consent for publication

Not applicable.

### Competing interests

The authors declare that they have no competing interests.

### References

1. Itakura E, Yamamoto H, Oda Y and Tsuneyoshi M: Detection and characterization of vascular endothelial growth factors and their receptors in a series of angiosarcomas. *J Surg Oncol* 97: 74-81, 2008.
2. Clifford CA, Mackin AJ and Henry CJ: Treatment of canine hemangiosarcoma: 2000 and beyond. *J Vet Intern Med* 14: 479-485, 2000.
3. Yonemaru K, Sakai H, Murakami M, Yanai T and Masegi T: Expression of vascular endothelial growth factor, basic fibroblast growth factor, and their receptors (flt-1, flk-1, and flg-1) in canine vascular tumors. *Vet Pathol* 43: 971-980, 2006.
4. Chappell WH, Steelman LS, Long JM, Kempf RC, Abrams SL, Franklin RA, Bāsecke J, Stivala F, Donia F, Fagone P, *et al.*: Ras/Raf/MEK/ERK and PI3K/PTEN/Akt/mTOR inhibitors: Rationale and importance to inhibiting these pathways in human health. *Oncotarget* 2: 135-164, 2011.

5. di Blasio L, Puliafito A, Gagliardi PA, Comunanza V, Somale D, Chiaverina G, Bussolino F and Primo L: PI3K/mTOR inhibition promotes the regression of experimental vascular malformations driven by PIK3CA-activating mutations. *Cell Death Dis* 9: 45, 2018.
6. Matsumura I, Mizuki M and Kanakura Y: Roles for deregulated receptor tyrosine kinases and their downstream signaling molecules in hematologic malignancies. *Cancer Sci* 99: 479-485, 2008.
7. Arbiser JL, Weiss SW, Arbiser ZK, Bravo F, Govindajaran B, Caceres-Rios H, Cotsonis G, Recavarren S, Swerlick RA and Cohen C: Differential expression of active mitogen-activated protein kinase in cutaneous endothelial neoplasms: Implications for biologic behavior and response to therapy. *J Am Acad Dermatol* 44: 193-197, 2001.
8. Kroll J and Waltenberger J: The vascular endothelial growth factor receptor KDR activates multiple signal transduction pathways in porcine aortic endothelial cells. *J Biol Chem* 272: 32521-32527, 1997.
9. Jiang X, Wang J, Deng X, Xiong F, Zhang S, Gong Z, Li X, Cao K, Deng H, He Y, *et al*: The role of microenvironment in tumor angiogenesis. *J Exp Clin Cancer Res* 39: 204, 2020.
10. Blasio A, Wang J, Wang D, Varodayan FP, Pomrenze MB, Miller J, Lee AM, McMahon T, Gyawali S, Wang HY, *et al*: Novel small-molecule inhibitors of protein kinase C epsilon reduce ethanol consumption in mice. *Biol Psychiatry* 84: 193-201, 2018.
11. Le Cras TD, Goines J, Lakes N, Pastura P, Hammill AM, Adams DM and Boscolo E: Constitutively active PIK3CA mutations are expressed by lymphatic and vascular endothelial cells in capillary lymphatic venous malformation. *Angiogenesis* 23: 425-442, 2020.
12. Dickerson EB, Thomas R, Fosmire SP, Lamerato-Kozicki AR, Bianco SR, Wojcieszyn JW, Breen M, Helfand SC and Modiano JF: Mutations of phosphatase and tensin homolog deleted from chromosome 10 in canine hemangiosarcoma. *Vet Pathol* 42: 618-632, 2005.
13. Tate G, Suzuki T and Mitsuya T: Mutation of the PTEN gene in a human hepatic angiosarcoma. *Cancer Genet Cytogenet* 178: 160-162, 2007.
14. Lahat G, Dhuka AR, Halleivi H, Xiao L, Zou C, Smith KD, Phung TL, Pollock RE, Benjamin R, Hunt KK, *et al*: Angiosarcoma: Clinical and molecular insights. *Ann Surg* 251: 1098-1106, 2010.
15. Murai A, Asa SA, Kodama A, Hirata A, Yanai T and Sakai H: Constitutive phosphorylation of the mTORC2/Akt/4E-BP1 pathway in newly derived canine hemangiosarcoma cell lines. *BMC Vet Res* 8: 128, 2012.
16. Tamburini BA, Trapp S, Phang TL, Schappa JT, Hunter LE and Modiano JF: Gene expression profiles of sporadic canine hemangiosarcoma are uniquely associated with breed. *PLoS One* 4: e5549, 2009.
17. Lequarre AS, Andersson L, Andre C, Fredholm M, Hitte C, Leeb T, Lohi H, Lindblad-Toh K and Georges M: LUPA: A European initiative taking advantage of the canine genome architecture for unravelling complex disorders in both human and dogs. *Vet J* 189: 155-159, 2011.
18. Espejo-Freire AP, Elliott A, Rosenberg A, Costa PA, Barreto-Coelho P, Jonczak E, D'amato G, Subhawong T, Arshad J, Diaz-Perez JA, *et al*: Genomic landscape of angiosarcoma: A targeted and immunotherapy biomarker analysis. *Cancers* 13: 4816, 2021.
19. Wang G, Wu M, Maloneyhuss MA, Wojcik J, Durham AC, Masson NJ and Royh DB: Actionable mutations in canine hemangiosarcoma. *PLoS One* 12: e0188667, 2017.
20. Arafah R and Samuels Y: PIK3CA in cancer: The past 30 years. *Semin Cancer Biol* 59: 36-49, 2019.
21. André F, Ciruelos E, Rubovszky G, Campone M, Loibl S, Rugo HS, Iwata H, Conte P, Mayer IA, Kaufman K, *et al*: Alpelisib for PIK3CA-mutated, hormone receptor-positive advanced breast cancer. *N Engl J Med* 380: 1929-1940, 2019.
22. Misdorp W; Armed Forces Institute of Pathology (U.S.); American Registry of Pathology; WHO Collaborating Center for Worldwide Reference on Comparative Oncology: Histological classification of mammary tumors of the dog and the cat. In: *International Histological Classification of Tumors of Domestic Animals*. Vol 7. 2nd series. Armed Forces Institute of Pathology in cooperation with the American Registry of Pathology and the World Health Organization Collaborating Center for Worldwide Reference on Comparative Oncology, Washington, DC, 1999.
23. Uyama R, Nakagawa T, Hong SH, Mochizuki M, Nishimura R and Sasaki N: Establishment of four pairs of canine mammary tumour cell lines derived from primary and metastatic origin and their E-cadherin expression. *Vet Comp Oncol* 4: 104-113, 2006.
24. Ghazanchaei A, Mansoori B, Mohammadi A, Biglari A and Baradaran B: Restoration of miR-152 expression suppresses cell proliferation, survival, and migration through inhibition of AKT-ERK pathway in colorectal cancer. *J Cell Physiol* 234: 769-776, 2019.
25. Madsen RR, Vanhaesebroeck B and Semple RK: Cancer-associated PIK3CA mutations in overgrowth disorders. *Trends Mol Med* 24: 856-870, 2018.
26. Kim JH: PIK3CA mutations matter for cancer in dogs. *Res Vet Sci* 133: 39-41, 2020.
27. Ney JT, Froehner S, Roesler A, Buettner R and Merkelbach-Bruse S: High-resolution melting analysis as a sensitive prescreening diagnostic tool to detect KRAS, BRAF, PIK3CA, and AKT1 mutations in formalin-fixed, paraffin-embedded tissues. *Arch Pathol Lab Med* 136: 983-992, 2012.
28. Beca F, Krings G, Chen YY, Hosfield EM, Vohra P, Sibley RK, Troxell ML, West RB, Allison KH and Bean GR: Primary mammary angiosarcomas harbor frequent mutations in KDR and PIK3CA and show evidence of distinct pathogenesis. *Mod Pathol* 33: 1518-1526, 2020.
29. Wang G, Wu M, Durham AC, Mason NJ and Roth DB: Canine oncopanel: A capture-based, NGS platform for evaluating the mutational landscape and detecting putative driver mutations in canine cancers. *Vet Comp Oncol* 20: 91-101, 2022.
30. Wang J, Zhao W, Guo H, Fang Y, Stockman SE, Bai S, Ng PK, Li Y, Yu Q, Lu Y, *et al*: AKT isoform-specific expression and activation across cancer lineages. *BMC Cancer* 18: 742, 2018.
31. Guo H, Gao M, Lu Y, Liang J, Lorenzi PL, Bai S, Hawke DH, Li J, Dogruluk T, Scott KL, *et al*: Coordinate phosphorylation of multiple residues on single AKT1 and AKT2 molecules. *Oncogene* 33: 3463-3472, 2014.
32. Dillon RL, Marcotte R, Hennessy BT, Woodgett JR, Mills GB and Muller WJ: Akt1 and akt2 play distinct roles in the initiation and metastatic phases of mammary tumor progression. *Cancer Res* 69: 5057-5064, 2009.
33. Ihle MA, Fassunke J, König K, Grunewald I, Schlaak M, Kreuzberg N, Tietze L, Schildhaus HU, Büttner R and Merkelbach-Bruse S: Comparison of high resolution melting analysis, pyrosequencing, next generation sequencing and immunohistochemistry to conventional Sanger sequencing for the detection of p.V600E and non-p.V600E BRAF mutations. *BMC Cancer* 14: 13, 2014.
34. Rascio F, Spadaccino F, Rocchetti MT, Castellano G, Stallone G, Netti GS and Ranieri E: The pathogenic role of PI3K/AKT pathway in cancer onset and drug resistance: An updated review. *Cancers* 13: 3949, 2021.
35. Fritsch C, Huang A, Chatenay-Rivauday C, Schnell C, Reddy A, Liu M, Kauffmann A, Guthy D, Erdmann D, De Pover A, *et al*: Characterization of the novel and specific PI3K $\alpha$  inhibitor NVP-BYL719 and development of the patient stratification strategy for clinical trials. *Mol Cancer Ther* 13: 1117-1129, 2014.
36. Im KS, Graef AJ, Breen M, Lindblad-Toh K, Modiano JF and Kim JH: Interactions between CXCR4 and CXCL12 promote cell migration and invasion of canine hemangiosarcoma. *Vet Comp Oncol* 15: 315-327, 2017.
37. Kim JH, Graef AJ, Dickerson EB and Modiano JF: Pathobiology of hemangiosarcoma in dogs: Research advances and future perspectives. *Vet Sci* 2: 388-405, 2015.
38. Kim KH, Chung WS, Kim Y, Kim KS, Lee IS, Park JY, Jeong HS, Na YC, Lee CH and Jang HJ: Transcriptomic analysis reveals wound healing of morus alba root extract by up-regulating keratin filament and CXCL12/CXCR4 signaling. *Phytother Res* 29: 1251-1258, 2015.
39. Zuo J, Wen M, Li S, Lv X, Wang L, Ai X and Lei M: Overexpression of CXCR4 promotes invasion and migration of non-small cell lung cancer via EGFR and MMP-9. *Oncol Lett* 14: 7513-7521, 2017.

